

## Old Dominion University ODU Digital Commons

---

Mathematics & Statistics Faculty Publications

Mathematics & Statistics

---

2017

# Fire, Ice, Water, and Dirt: A Simple Climate Model

John Kroll

Old Dominion University, [jkroll@odu.edu](mailto:jkroll@odu.edu)

Follow this and additional works at: [https://digitalcommons.odu.edu/mathstat\\_fac\\_pubs](https://digitalcommons.odu.edu/mathstat_fac_pubs)

 Part of the [Applied Mathematics Commons](#), and the [Engineering Physics Commons](#)

---

### Repository Citation

Kroll, John, "Fire, Ice, Water, and Dirt: A Simple Climate Model" (2017). *Mathematics & Statistics Faculty Publications*. 43.  
[https://digitalcommons.odu.edu/mathstat\\_fac\\_pubs/43](https://digitalcommons.odu.edu/mathstat_fac_pubs/43)

### Original Publication Citation

Kroll, J. (2017). Fire, ice, water, and dirt: A simple climate model. *Chaos: An Interdisciplinary Journal of Nonlinear Science*, 27(7), 073101. doi:10.1063/1.4991383

This Article is brought to you for free and open access by the Mathematics & Statistics at ODU Digital Commons. It has been accepted for inclusion in Mathematics & Statistics Faculty Publications by an authorized administrator of ODU Digital Commons. For more information, please contact [digitalcommons@odu.edu](mailto:digitalcommons@odu.edu).

## Fire, ice, water, and dirt: A simple climate model

John Kroll

Citation: *Chaos* **27**, 073101 (2017); doi: 10.1063/1.4991383

View online: <http://dx.doi.org/10.1063/1.4991383>

View Table of Contents: <http://aip.scitation.org/toc/cha/27/7>

Published by the [American Institute of Physics](#)

---

### Articles you may be interested in

[Constructing an autonomous system with infinitely many chaotic attractors](#)

*Chaos: An Interdisciplinary Journal of Nonlinear Science* **27**, 071101 (2017); 10.1063/1.4986356

[Information theory and robotics meet to study predator-prey interactions](#)

*Chaos: An Interdisciplinary Journal of Nonlinear Science* **27**, 073111 (2017); 10.1063/1.4990051

[Public goods games on adaptive coevolutionary networks](#)

*Chaos: An Interdisciplinary Journal of Nonlinear Science* **27**, 073107 (2017); 10.1063/1.4991679

[Fisher information and Rényi entropies in dynamical systems](#)

*Chaos: An Interdisciplinary Journal of Nonlinear Science* **27**, 073104 (2017); 10.1063/1.4993168

[Nonlinear resonances and multi-stability in simple neural circuits](#)

*Chaos: An Interdisciplinary Journal of Nonlinear Science* **27**, 013118 (2017); 10.1063/1.4974028

[On the sighting of unicorns: A variational approach to computing invariant sets in dynamical systems](#)

*Chaos: An Interdisciplinary Journal of Nonlinear Science* **27**, 063102 (2017); 10.1063/1.4983468

---

Welcome to a

Smarter Search 

PHYSICS  
TODAY

with the redesigned  
*Physics Today Buyer's Guide*

Find the tools you're looking for today!

## Fire, ice, water, and dirt: A simple climate model

John Kroll

*Department of Mathematics, Old Dominion University, Norfolk, Virginia 23529, USA*

(Received 7 March 2016; accepted 20 June 2017; published online 10 July 2017)

A simple paleoclimate model was developed as a modeling exercise. The model is a lumped parameter system consisting of an ocean (water), land (dirt), glacier, and sea ice (ice) and driven by the sun (fire). In comparison with other such models, its uniqueness lies in its relative simplicity yet yielding good results. For nominal values of parameters, the system is very sensitive to small changes in the parameters, yielding equilibrium, steady oscillations, and catastrophes such as freezing or boiling oceans. However, stable solutions can be found, especially naturally oscillating solutions. For nominally realistic conditions, natural periods of order 100kyrs are obtained, and chaos ensues if the Milankovitch orbital forcing is applied. An analysis of a truncated system shows that the naturally oscillating solution is a limit cycle with the characteristics of a relaxation oscillation in the two major dependent variables, the ocean temperature and the glacier ice extent. The key to getting oscillations is having the effective emissivity decreasing with temperature and, at the same time, the effective ocean albedo decreases with increasing glacier extent. Results of the original model compare favorably to the proxy data for ice mass variation, but not for temperature variation. However, modifications to the effective emissivity and albedo can be made to yield much more realistic results. The primary conclusion is that the opinion of Saltzman [Clim. Dyn. **5**, 67–78 (1990)] is plausible that the external Milankovitch orbital forcing is not sufficient to explain the dominant 100kyr period in the data. *Published by AIP Publishing.* [<http://dx.doi.org/10.1063/1.4991383>]

**Over the last million years or so, data show that the primary ice age period is about 100kyrs. One of the Milankovitch orbital forcing periods is around this period, but why this relatively weak forcing should dominate is not apparent. In this paper, a quite simple model that yields such a dominant period is developed and analyzed. This would indicate the plausibility of the existence of an underlying natural period in the nonlinear dynamics that produces the observed period. The uniqueness of the model lies in its relative simplicity.**

### I. INTRODUCTION

A challenge in mathematical modeling is to try to reduce a very complicated problem to its essence to obtain relatively simple yet useful results. Such a problem is the evolution of the ice mass and temperature of the earth in the last  $5 \times 10^6$  years. Well known proxy data of the ice mass variation (Hays *et al.*, 1976) and deep ocean temperature variation (Hansen and Sato, 2011) show fairly obvious, nearly periodic, “spikey” behavior. Modeling this behavior in any precise way is very difficult, but the oscillations suggest that there might be fairly simple mathematical models to give useful approximate results. So we start the process with the basic elements involved: fire (the sun), ice (the glaciers and sea ice), water (the ocean and vapor), and dirt (the land). We then bring all these elements together in a lumped parameter system using basic conservation principles of mass, volume, and heat and apply the basic heat transfer mechanisms of radiation, convection, and conduction. We add to this the Milankovitch astronomical forcing to complete the model. We have a number of unknown parameters that are evaluated

so as to obtain the behavior of the proxy data. The model is a relatively simple nonlinear system that yields interesting results.

The genesis of this work was a proposal by Denny Kirwan for a thesis problem to a graduate student in applied mathematics. The proposal was to add a few more simple concepts to combine the simplicity of a toy climate model such as that of Posmentier (1990), which was analyzed by Toner and Kirwan (1994), with the concept of “Daisyworld,” first proposed by Watson and Lovelock (1983) and further developed by Saunders (1994). The “Daisyworld” concept speculated on the biological effects on climate due to changes in the albedo caused by differing biota which in turn can feedback to affect the biota. I became interested in it as an example for a mathematical modeling class. How good of a model could be devised using a basic understanding of physics without any real expert knowledge of climatology? Thus, starting with some of the basic concepts (some put forth originally by Kirwan), using other basic concepts of the physics of heat and a couple of rather *ad hoc* relationships, the model of this paper was developed.

Subsequent to the proposal of “Daisyworld,” many other investigators went on to develop the concept which is reviewed by Wood *et al.* (2008). However, the low dimensional climate model that is developed, without any “Daisyworld” modifications, is of sufficient interest that at this time we will study only it in this paper. This present model is in the stream of relaxation oscillation models, beginning with Welander (1982) for the ocean, through the seminal low dimensional climate modeling of Saltzman (Saltzman *et al.*, 1981 and 1984) to the climate modeling of Crucifix and Rougier (2009). Crucifix (2012) summarizes

this development through 2011 and makes the case for the continued usefulness of low dimensional models even though much more complex ones can be developed with the increase in computer power.

The proxy data show an approximately periodic growth and decay of the evolution of the ice mass. Going back approximately two million years, the period has gone from around 40kyrs, changing rather abruptly to 100kyrs from about 800kyrs ago to the present. It would seem that the fact that there is Milankovitch planetary forcing at these periods would be an obvious explanation for these periods. However, the amplitude of the 100kyrs forcing is weak and it is not obvious why there exist such large oscillations in the ice mass. The Milankovitch forcing is important but also so is the dynamics of the underlying system. It is still not precisely known how the combination of forcing and dynamics produces what has been observed. Since the physics are extremely complicated with time scales so long, many proposed models tend to emphasize either the forcing or the dynamics. For example, the paper by [Tziperman \*et al.\* \(2006\)](#) emphasizes the forcing in considering the interaction of the forcing periods with a nonlinear system to produce phase locking. On the other hand, the work of [Saltzman \(2002\)](#) emphasizes the dynamics and produces realistic periods without the forcing.

The thrust of recent investigations is to be able to predict “tipping points” when one oscillation regime transitions to another, such as the 41kyr to 100kyrs change. This is relevant today with the possibility of man-made global warming pushing the climate into a new nonbeneficial regime. The usual suspect in such a change is a bifurcation produced by the change of some parameter in the dynamical system. For example, it is a slow, tectonic scale, change in CO<sub>2</sub> concentration for [Saltzman \(2002\)](#) and [Paillard and Parrenin \(2004\)](#). For more complex models, it is not clear that there is one such parameter. Recently, [Bathiany \*et al.\* \(2016\)](#) have proposed going beyond bifurcation to consider more complex models to see if reliable triggers can be found for tipping points.

The primary purpose here is not to resolve the deeper questions or find tipping points, but to develop a simple modeling idea and see what happens. The model is a low dimensional relaxation model that emphasizes the dynamics rather than the forcing. The uniqueness of our model is that it is simple, and has fairly well understood physical bases. I believe it is interesting because it yields surprisingly realistic results and the modeling process in itself is interesting.

The data of most interest are that of the past 800kyrs which show for the variation of ice mass the characteristic “spikey” character with a slow growth and a swift melt, while deep ocean temperature slowly decreases and then swiftly increases. This slow and fast change is a characteristic of a relaxation oscillation. There is also a clear dominant period of around 100kyrs. Spectra of data also show this dominant period and lesser peaks around 20kyrs and 40kyrs. Of course, all of these dominant periods correspond to the Milankovitch orbital forcing periods and are expected. However, it was the opinion of [Saltzman \(1990\)](#) that orbital forcing is not sufficient for the dominant 100kyr period even

though one of the forcing periods is 100kyrs. He believed that nonlinear dynamics plays a large role and results of this paper tend to confirm this.

In Sec. II, we develop the model. In Sec. III, we summarize the equations of the system, the forcing of the system, and values of the parameters. In Sec. IV, we calculate and discuss results. In Sec. V, we develop and discuss a truncated system to better analyze the basic system and to see how we can modify the model to get better results. In Sec. VI, we summarize and state the conclusions.

## II. THE MODEL

We assume a lumped parameter system: two lumps of ice (glacier and sea ice), one lump of dirt (dry land), and one lump of water (ocean) as shown schematically in Fig. 1. The dry land and the ocean are confined to their own sectors of the earth with glacier ice on the poleward part of the land sector and sea ice on the poleward part of the ocean sector. We assume that the earth is hemispherically symmetric (which is clearly not realistic). We do not consider either the mass or heat content of the atmosphere but consider it only as a medium to transfer heat. The sum of the areas of the ocean ( $s_o$ ), the land ( $s_l$ ), the glacier ( $s_g$ ), and the sea ice ( $s_s$ ) of course equals the total area of the earth ( $s$ ). We assume that the mass of water is conserved, and, if we neglect the mass of water vapor and assume that the densities of liquid and ice are approximately the same, then we can assume that the total volume of liquid and solid water ( $V_w$ ) is conserved so that we have:

$$\delta_g s_g + \delta_s s_s + \delta_o (s_o + s_s) = V_w, \quad (1)$$

where the  $\delta$ 's are average thickness or depth. The approximate values of these quantities on the earth today can be found in [Trenberth \(1992\)](#) and [Peixoto and Oort \(1992\)](#):  $\delta_g \approx 2280$  m,  $\delta_s \approx 2$  m,  $\delta_o \approx 3800$  m,  $s_g \approx 0.029$  s,  $s_s \approx 0.048$  s,  $s_o \approx 0.71$  s, and  $V_w \approx 0.71 \delta_o s$ , where  $s \approx 4\pi(6300)^2$  km<sup>2</sup>.

We first apply the conservation of mass to the glacier

$$\dot{m}_g = \dot{m}_{gp} - \dot{m}_{gm}, \quad (2)$$

where  $\dot{m}_g$  is the rate of accumulation of mass of the glacier,  $\dot{m}_{gp}$  is the precipitation rate onto the glacier, and  $\dot{m}_{gm}$  is the “melting” rate of the glacier, which includes all manner of

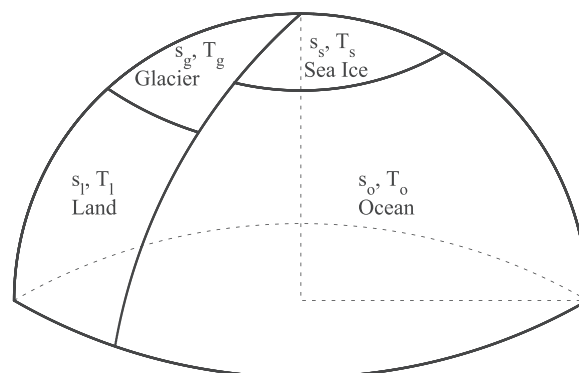


FIG. 1. Schematic diagram of the area sectors of ocean ( $s_o$ ), land ( $s_l$ ), glacier ( $s_g$ ), and sea ice ( $s_s$ ).

ablation. The precipitation is assumed to vary jointly with the respective areas,  $\dot{m}_{gp} = BF_w(T_o)s_g s_o$ , where  $B$  is a constant to be determined by data for present conditions and  $F_w(T_o)$  represents the variation of the amount of water vapor in the air as a function of the ocean temperature,  $T_o$ . We assume that this function is given approximately by  $F_w(T_o) = 5 + 0.367(T_o - T_f)e^{0.0285(T_o - T_f)}$ ,  $T_f \leq T_o \leq 100$ , where  $T_f$  is the temperature of fusion ( $\simeq -3^\circ\text{C}$ ). The coefficients are found from the relationship for vapor pressure as a function of temperature.

The melting is assumed to behave analogously to a melting lump of ice where any heat applied will raise the temperature until it reaches an effective ‘‘melting’’ temperature,  $T_m$ , and thereafter any additional added heat will melt the ice. Thus,  $\dot{m}_{gm} = H_g/L_g$  if  $T_g = T_m$  and the net heat flow to the glacier,  $H_g$ , is positive where  $L_g$  is the latent heat of fusion. However, if  $H_g$  is negative, the glacier does not gain ice from this term. So  $\dot{m}_{gm} = 0$  if  $T_g < T_m$  or  $H_g < 0$ . The mass accumulation rate for the sea ice,  $\dot{m}_s$ , is very similar except we can accommodate the net heat flow being negative to produce freezing and an increase of sea ice if  $T_o$  goes to the freezing temperature. (We might consider the latent heat of fusion for the glacier  $L_g$  and that for the sea ice,  $L_s$ , to be effectively different, but we did not and let them both be the regular value of  $334 \text{ J g}^{-1}$ .) An estimate of the present value of  $\dot{m}_{gp}$  is  $2740 \times 10^{12} \text{ kg/yr}$  from [Trenberth \(1992\)](#). This is the approximate rate for melting also since  $\dot{m}_g$  is about zero at present. We assume that this rate converted to the rate per unit area is the same for the sea ice. We also assume that the effective ‘‘melting’’ temperature,  $T_m$ , will not be the freezing temperature,  $T_f = 271 \text{ K}$ , but something less than this.

The heat transfer term,  $H_g$ , in  $\dot{m}_{gm}$  is given by

$$H_g = s_g \left[ S_g(1 - A_g) - \epsilon_e \sigma T_g^4 + h_{s_o}(T_o - T_g) + h_{s_s}(T_s - T_g) + h_{s_l}(T_l - T_g) \right], \quad (3)$$

where the heat transfer from one area to another is assumed to vary with the temperature difference and vary jointly with the areas. The first term is net input of heat (radiation from the sun minus that reflected, represented by the albedo,  $A_g$ ). The second is the heat radiated away from the glacier where  $\sigma \simeq 5.67 \times 10^{-8} \text{ Wm}^{-2} \text{ K}^{-4}$  is the Stefan-Boltzmann constant. An effective emissivity,  $\epsilon_e$ , is assumed to account for the atmosphere. It would be 1 for a vacuum, but less than one with an atmosphere containing water vapor. The last three terms represent the heat transfer via the atmosphere from the ocean, the sea ice, and the land to the glacier, respectively, where  $h$  is an effective heat transfer coefficient within the atmosphere. The forms for the heat transfer terms for the sea ice,  $H_s$ , the ocean,  $H_o$ , and the land,  $H_l$ , will be similar to that of (3), changing to the appropriate subscripts. We will discuss albedos, emissivity, and heat transfer coefficients further below.

The conservation of heat applied to the glacier yields

$$m_g c \dot{T}_g = R_g = H_g + \dot{m}_{gp}c(T_o - T_g), \text{ if } R_g < 0 \text{ or } T_g < T_m, \\ T_g = T_m, \text{ otherwise,} \quad (4)$$

where  $\dot{T}_g$  is the rate of change of the glacier temperature,  $T_g$ , and  $c$  is the heat capacity, which is assumed the same for ocean and ice (1 in cgs units). Again the model of the glacier is that of a block of ice, which changes temperature only if its temperature,  $T_g$ , is less than the effective melting temperature,  $T_m$ , or, if  $T_g$  is equal to  $T_m$ , decreases if  $R_g < 0$ . The second term on the right which is the sensible heat from the moisture originally from the ocean to the glacier should be negligible in most cases to  $H_g$ . We assume that the mass of the glacier is given by  $m_g = \rho_g \delta_g s_g$ , where  $\rho_g$  is the density of the ice (which we assume is the same as for the sea ice and the water, = 1 cgs units). Thus, we initially assume that as the glacier grows, it spreads out in area but does not thicken, a very gross assumption which we will modify later.

The equivalent equation for the sea ice is simply that the sea ice temperature,  $T_s$ , is constant and equal to its melting temperature which is assumed to be  $T_f$ . Thus, we are assuming that the change in temperature of the sea ice is unimportant with the heat transfer to the sea ice,  $H_s$ , either melting it when positive or freezing it to expand it when negative. As with the glacier, we assume that the sea ice only changes in area and not in thickness, a much better assumption for sea ice than glacier.

The conservation of heat for the ocean yields

$$m_o c \dot{T}_o = H_o + \left( \frac{s_o}{s_o + s_l} \right) L_v (\dot{m}_{gp} + \dot{m}_{sp}) - L_{ev} (\dot{m}_{gp} + \dot{m}_{sp}) - \dot{m}_{gm} c_p (T_o - T_g) - \dot{m}_{sm} c_p (T_o - T_s), \quad (5)$$

where the first term on the right is a heat transfer term for the ocean, analogous to that for the glacier [Eq. (3)], the second term is the fraction going into the ocean of the latent heat released into the atmosphere as precipitation falls on the ice, the third term is latent heat lost by the ocean in evaporation, and the fourth and fifth terms represent heat lost in heating up water melted from the ice. These last terms should be much less than the latent heat terms and can probably be neglected. In the above,  $L_v = 2835 \text{ J g}^{-1}$  is the latent heat of evaporation plus the latent heat of fusion;  $L_{ev} = 2501 \text{ J g}^{-1}$  is the latent heat of evaporation. Since the mass of the ocean,  $m_o$ , also includes the part under the sea ice,  $m_o = \rho_o \delta_o (s_o + s_s)$ .

The equivalent equation for the conservation of heat for the land is similar to that above for the ocean but without the three last terms. The mass of the land is given by  $m_l = \rho_l \delta_l s_l$  which is certainly smaller than the mass of the whole earth. The density,  $\rho_l$ , and the thickness,  $\delta_l$ , along with the heat capacity of the land,  $c_l$ , are quite nebulous and are assumed to be some ‘‘effective’’ values.

Let us now use the fractional area:  $\alpha_n = s_n/s$ , where the subscript  $n$  is  $g$ ,  $s$ ,  $o$ , or  $l$ . The fractional area of the ocean can then be found in terms of that of the glacier and sea ice using the conservation of water (1)

$$\alpha_o = V_w / (\delta_o s) - \delta_g \alpha_g / \delta_o - \alpha_s. \quad (6)$$

The fractional area of the land is simply

$$\alpha_l = 1 - \alpha_o - \alpha_g - \alpha_s. \quad (7)$$

Maximum values for  $\alpha_g$  and  $\alpha_s$  will be useful. Since  $\alpha_o + \alpha_s \geq 0$ , from (6),  $\alpha_g \leq V_w/(\delta_g s) = \alpha_{gm1}$ . But if  $\delta_g \leq \delta_o$ , since  $\alpha_l \geq 0$ , then  $\alpha_g \leq (1 - \frac{V_w}{s\delta_o})/(1 - \frac{\delta_g}{\delta_o}) = \alpha_{gm2}$ . So the maximum of  $\alpha_g$  is given by  $\alpha_{gmax} = \text{Min}(\alpha_{gm1}, \alpha_{gm2})$  and, since  $\alpha_o \geq 0$ , the maximum of  $\alpha_s$  is given by  $\alpha_{smax} = V_w/(\delta_o s) - \delta_g \alpha_g / \delta_o$ , from (6).

The radiation per unit area of earth surface from the sun depends on the latitude. Since we have symmetry, we consider a hemisphere. The average radiation per unit area on the surface of a spherical cap with area,  $s_s$ , for the polar angle,  $\phi$ , ( $\pi/2 - \text{latitude}$ ) from 0 to  $\phi_o$  is given by  $S_s = \frac{A_c}{s_c} S_c$  where  $A_c$  is the projected area of  $s_{sc}$  on the cross-sectional disk of the sphere, and  $S_c$  is the total radiation per unit area from the sun ( $\approx 1360 \text{ W m}^{-2}$ ) called the solar constant. (We assume that this is true even if  $s_s$  is not the whole cap but only a fractional sector.) These areas can be calculated in terms of the polar angle,  $\phi_o$ , of the polar cap

$$A_c = 2 \int_0^{\phi_o} \int_{R \frac{\cos \phi_o}{\cos \phi}}^R r dr d\phi = R^2 [\phi_o - \sin \phi_o \cos \phi_o]$$

and

$$s_s = 2\pi \int_0^{\phi_o} R^2 \sin \phi d\phi = 2\pi R^2 (1 - \cos \phi_o), \quad (8)$$

where  $R \approx 6300 \text{ km}$  is the radius of the earth. It is important to note that  $\alpha_s = 1 - \cos \phi_o$ . We can then show that the average radiation per unit area onto the sea ice is given by

$$S_s = S_c (\phi_o - \sin \phi_o \cos \phi_o) / 2\pi \alpha_s. \quad (9)$$

We will replace  $\alpha_s$  with  $\bar{\alpha}_s = \frac{\alpha_s}{\alpha_{smax}}$  [and  $\phi_o = \cos^{-1}(1 - \bar{\alpha}_s)$ ] since the sea ice will not occupy a whole spherical cap but be confined to the surface of a sector of a sphere. Replacing the subscript  $s$  with  $g$ , we have the analogous expression for  $S_g$  for the glacier in terms of  $\bar{\alpha}_g = \frac{\alpha_g}{\alpha_{gmax}}$ .

In a similar manner, the same can be done to approximate the average solar radiation per unit area on the ocean,  $S_o$ , and on the land,  $S_l$

$$S_o = \frac{\left(\frac{\pi}{2} R^2 - A_c\right)}{s_o} = S_c (\pi/2 - \phi_o + \sin \phi_o \cos \phi_o) / 2\pi \alpha_o. \quad (10)$$

Replacing the subscript  $o$  with  $l$ , we have the analogous expression for the land.

Let us now look at some modifications:

Modification (1): The axis of the earth, of course, is not perpendicular to the ecliptic plane, but having an inclination,  $\beta_m$ , of about  $23^\circ$ . So every spot on earth gets some sun. Also, we would like to put the ‘‘wobbles’’ of the Milankovitch periods into the model in a fairly realistic manner. From the point of view from the sun, the apparent inclination angle ( $\beta$ ) varies from 0 to  $\beta_m(0.4 \text{ rad})$  as the earth revolves about the sun. Doing the same sort of calculation (though somewhat more complicated) for  $A_c$  as was done above (the case for  $\beta = 0$ ), we get for any  $\beta$

$$A_c = \left\{ \begin{array}{ll} \sin^2 \phi_o \sin \beta + \frac{2}{\pi} D, & \phi_o > \beta \\ \sin^2 \phi_o \sin \beta, & \phi_o < \beta \end{array} \right\}, \quad (11)$$

where  $D = \cos^{-1}\left(\frac{\cos \phi_o}{\cos \beta}\right) - \sin \beta \sin \phi_o \cos^{-1}\left(\frac{\tan \beta}{\tan \phi_o}\right) + (\cos \phi_o \tan^2 \beta - \frac{\cos \phi_o}{\cos^2 \beta}) \sqrt{\cos^2 \beta - \cos^2 \phi_o}$ .

The above function for  $A_c$  should be averaged over one revolution around the sun over the angle  $\theta$ , on the ecliptic plane, using the fact that  $\beta(\theta) = \tan \beta_m \sin \theta$ . But this would seem to be overly complicated, so we will just replace  $\beta$  with  $\beta_a$ , the average value of  $\beta$  over one revolution, i.e.,  $\beta_a = \frac{2}{\pi} \int_0^{\frac{\pi}{2}} \beta(\theta) d\theta \approx 0.26 \text{ rad}$ . So the modified value for  $A_c$  is (11) with  $\beta_a$  replacing  $\beta$ . Actually, introducing  $\beta$  turns out not to be crucial to the behavior of the model. Setting  $\beta = 0$  seemed to have a little qualitative effect.

Modification (2): There are some realistic modifications to the heat transfer that can be made. The heat transfer between the ocean and the sea ice is much more intimate than just that via the atmosphere as represented by the forms for  $H_o$  and  $H_s$  given previously [analogous to  $H_g$  given by (3)]. So we will add to  $H_s$  (and subtract from  $H_o$ ) a heat transfer term of the form  $h_{so} \alpha_s \alpha_o (T_{o\phi} - T_s)$ , where  $h_{so}$  is this special heat transfer coefficient between the ocean and the sea ice and  $T_{o\phi}$  is the approximate temperature of the ocean at the latitude,  $\phi$ , where the sea ice begins.

The variation of  $T_{o\phi}$  with latitude is approximated by the present variation of sea surface temperature from the equator to the pole. In terms of  $\alpha_s$  rather than latitude, this variation is approximated as

$$\frac{T_{o\phi} - T_f}{T_{oq} - T_f} = 1 - (1 - \bar{\alpha}_s)^2, \quad (12)$$

where  $T_{oq}$  is the approximate temperature at the equator for the ocean (and is a variable). We are using the average ocean temperature,  $T_o$ , as one of our main dependent variables so we need  $T_{o\phi}$  in terms of  $T_o$ . We first note that for the average over  $\bar{\alpha}_o = 1 - \bar{\alpha}_s$ ,

$$T_o = \frac{1}{1 - \bar{\alpha}_s} \int_{\bar{\alpha}_s}^1 T_{o\phi} d\bar{\alpha}'_s = T_{oq} - \frac{1}{3} (T_{oq} - T_f) (1 - \bar{\alpha}_s)^3$$

can be found in terms of  $T_{oq}$ . Then we eliminate  $T_{oq}$  in (12) to find

$$T_{o\phi} = \left[ T_o - \frac{1}{3} T_f (1 - \bar{\alpha}_s)^3 \right] \frac{\left[ 1 - (1 - \bar{\alpha}_s)^3 \right]}{\left[ 1 - \frac{1}{3} (1 - \bar{\alpha}_s)^3 \right]} + T_f (1 - \bar{\alpha}_s)^2. \quad (13)$$

For the sake of symmetry, we can do the same thing for a special heat transfer connection between the land and the glacier where we add to  $H_g$  (and subtract from  $H_l$ ) a heat transfer term of the form  $h_{gl} \alpha_g \alpha_l (T_{l\phi} - T_g)$ . The form of (13) will apply to  $T_{l\phi}$  with the appropriate change in subscripts (i.e.,  $l$  for  $o$  and  $g$  for  $s$ ). However, we expect the heat transfer coefficient,  $h_{gl}$ , between the land and the glacier to be much less than that between the ocean and the sea ice,  $h_{so}$ ,

because the land is not convecting heat beneath the glacier as the ocean is beneath the sea ice.

Modification (3): Instead of assuming that the glacier is a constant height, we will assume that the height varies directly with the square root of the surface area. So the water mass onto the glacier increases both its height and area. In terms of the volume rate  $\left(\frac{dV}{dt}\right)$ , we then have  $\dot{\alpha}_g \propto \frac{1}{\sqrt{\alpha_g}} \frac{dV}{dt}$ .

Since we do not have an atmosphere, we will model the greenhouse effect and the reflective effect of the atmosphere by modifying the emissivity and the albedos. The emissivity of a black body is one, and for most materials, it is close to one. We will modify the emissivity to form an “effective” emissivity,  $\epsilon_e$ , which will be less than one, that will account for the radiation being trapped in the atmosphere as a function of the amount of greenhouse gasses (mostly water vapor) in the atmosphere. We will also assume that the nominal real values for the albedos are modified by the atmosphere.

It will turn out that the two most important dependent variables will be  $T_o$  and  $\alpha_g$ . (We will verify this later.) So we will assume that the emissivity and the ocean albedo are functions of  $T_o$  and  $\alpha_g$ . An increase in  $T_o$  increases the amount of water vapor in the atmosphere, which should decrease  $\epsilon_e$  (greenhouse effect). At the same time, there should be an increase in clouds, which may or may not increase the albedo. It is more unclear how a change in  $\alpha_g$  would independently influence these parameters, but we will consider the possibility.

Since we have no idea what these functions are, we will simply assume that they are linear variations about fixed equilibrium values, i.e.,

$$\epsilon_e = \epsilon_{ei} + \epsilon_T(T_o - T_{oi}) + \epsilon_\alpha(\alpha_g - \alpha_{gi}), \quad (14)$$

where  $\epsilon_{ei}$  is the equilibrium value of  $\epsilon_e$ , and  $T_{oi}$ ,  $\alpha_{gi}$  the equilibrium values of  $T_o$  and  $\alpha_g$ . The variations,  $\epsilon_T$  and  $\epsilon_\alpha$ , are constants. We assume that this emissivity is the same for ocean, land, and glacier. The albedo is a measure of the reflectivity of a surface. We are assuming that the atmosphere above the surface is included with the surface as part of the effective albedo of that surface which should increase it somewhat. As with the emissivity, we will assume that the albedo of the ocean,  $A_o$  (and the albedo of the land,  $A_l$ ), varies linearly with  $T_o$  and  $\alpha_g$ , but we do not know precisely how, so we assume a variation like that for the emissivity

$$A_o = A_{oi} + A_T(T_o - T_{oi}) + A_\alpha(\alpha_g - \alpha_{gi}), \quad (15)$$

where  $A_{oi}$  is the value of  $A_o$  at equilibrium and  $A_T$  and  $A_\alpha$  are constants. Later we will modify (14) and (15) to produce more realistic results.

For the albedo of the land,  $A_l$ , is assumed to be a factor (greater than one) of  $A_o$ . For the albedos of the ice, we neglect any changes due to the atmosphere, but we assume that as the ice moves down closer to the equator that puddling begins to occur which would decrease the albedo. So we assume that the albedo of the glacier,  $A_g$ , and the sea ice,  $A_s$ , decreases linearly with  $\alpha_g$  and  $\alpha_s$ , respectively

$$A_g = A_{gi} - a(\alpha_g - \alpha_{gi}), \quad (16)$$

$$A_s = A_{si} - a(\alpha_s - \alpha_{si}), \quad (17)$$

where  $a$  is a constant.

### III. THE SYSTEM OF EQUATIONS

We have five dependent variables in the model. They are  $\alpha_g$  and  $\alpha_s$ , which are dimensionless and  $T_o, T_l$ , and  $T_g$  in units of K. The independent variable is of course time,  $t$ , in years. The system of differential equations is

$$\frac{d\alpha_g}{dt} = \frac{C_1}{\delta_g} \left[ BF_w \alpha_g \alpha_o - \frac{H_g}{L_g} U(H_g) U(T_g - T_m) \right] \sqrt{\frac{\alpha_{gi}}{\alpha_g}}, \quad (18a)$$

$$\begin{aligned} \frac{d\alpha_s}{dt} = & \frac{C_1}{\delta_s} \left[ BF_w \alpha_s \alpha_o - \frac{H_s}{L_s} \right] U(T_o - T_f) \\ & - \frac{C_1}{\delta_s L_s} [H_o + \alpha_o BF_w (\alpha_o + \alpha_s)] U(T_f - T_o), \end{aligned} \quad (18b)$$

$$\begin{aligned} \frac{dT_o}{dt} = & \frac{C_2}{\delta_o (\alpha_o + \alpha_s)} \left\{ H_o - C_3 \left[ \frac{H_g}{L_g} (T_o - T_g) + \frac{H_s}{L_s} (T_o - T_s) \right] \right. \\ & \left. + \alpha_o BF_w (\alpha_s + \alpha_g) \left( \frac{\alpha_o L_v}{\alpha_o + \alpha_l} - L_e \right) \right\} \\ & * U(T_o - T_f) U(373 - T_o), \end{aligned} \quad (18c)$$

$$\frac{dT_l}{dt} = \frac{C_2}{\delta_l} \left[ \frac{H_l}{\alpha_l} + \frac{\alpha_o}{\alpha_o + \alpha_l} BF_w (\alpha_o + \alpha_s) \right], \quad (18d)$$

$$\frac{dT_g}{dt} = \frac{C_2}{\delta_g} \left[ \frac{H_g}{\alpha_g} + C_3 BF_w \alpha_o (T_o - T_g) \right] U(T_m - T_g), \quad (18e)$$

where the heat transfer terms are given by

$$\begin{aligned} H_g = & \alpha_g \{ S_g (1 - A_g) - \epsilon_e \sigma T_g^4 + h [\alpha_s (T_s - T_g) \\ & + \alpha_o (T_o - T_g) + \alpha_l (T_l - T_g)] + h_{gl} \alpha_l (T_{\phi l} - T_g) \}, \end{aligned} \quad (19a)$$

$$\begin{aligned} H_s = & \alpha_s \{ S_s (1 - A_s) - \epsilon_e \sigma T_s^4 + h [\alpha_g (T_g - T_s) \\ & + \alpha_o (T_o - T_s) + \alpha_l (T_l - T_s)] + h_{so} \alpha_o (T_{\phi o} - T_s) \}, \end{aligned} \quad (19b)$$

$$\begin{aligned} H_o = & \alpha_o \{ S_o (1 - A_o) - \epsilon_e \sigma T_o^4 + h [\alpha_s (T_s - T_o) \\ & + \alpha_g (T_g - T_o) + \alpha_l (T_l - T_o)] - h_{so} \alpha_s (T_{\phi o} - T_s) \}, \end{aligned} \quad (19c)$$

$$\begin{aligned} H_l = & \alpha_l \{ S_l (1 - A_l) - \epsilon_e \sigma T_l^4 + h [\alpha_s (T_s - T_l) \\ & + \alpha_o (T_o - T_l) + \alpha_g (T_g - T_l)] - h_{gl} \alpha_g (T_{\phi l} - T_g) \}, \end{aligned} \quad (19d)$$

and the quantities in the above equations were defined in Sec. II. The symbol  $\bar{\delta}_l$  in (18d) is the product of the specific heat, the specific density, and the effective depth for the land. The constants  $C_1, C_2$ , and  $C_3$  are conversion factors:  $C_1 = \text{seconds per year/density of water in grams per cubic meter} = 31.5 \frac{\text{s m}^3}{\text{yr g}}$ ,  $C_3 = \text{heat capacity of water} = 4.2 \frac{\text{J}}{\text{g K}}$ , and  $C_2 = C_1/C_3 = 7.51 \text{ m}^3 \text{ s K/J yr}$ .

The step function  $U()$  is defined to be 1 for the argument  $\geq 0$  and 0 for the argument  $< 0$ . It is used to model the glacier as a block of ice. In (18e), the temperature of the glacier is not allowed to exceed  $T_m$ , and in (18a), the heat flow to the glacier ( $H_g$ ) can only melt ice and not produce it. It is also used so that the ocean temperature cannot exceed boiling or decrease below freezing in (18c).

The system is forced by the orbital perturbations: the precession with period,  $P_p \approx 22$ kyrs, the obliquity with period,  $P_o \approx 41$ kyrs, and the eccentricity with period,  $P_e \approx 100$ kyrs. We assume that the precession and obliquity will perturb the inclination angle,  $\beta_a$ . For simplicity, we assume that all the forcings perturb  $\beta_a$ , and thus, we assume  $\beta_a = \beta_{ao} + b_p \sin\left(\frac{2\pi}{P_p}t\right) + b_o \sin\left(\frac{2\pi}{P_o}t\right) + b_e \sin\left(\frac{2\pi}{P_e}t\right)$ . The approximate periods of the forcing are well known, but the amplitude of the forcing is not. From [Berger and Loutre \(1991\)](#) and [Broecker \(1993\)](#), the amplitude of the obliquity,  $b_o$ , is about  $\frac{1.25\pi}{180}$  with that of the precession,  $b_p$ , about the same and that of the eccentricity,  $b_e$ , being a third less.

We have many parameters. Some are “hard” in that we know them exactly or at least fairly well. Some are “semi-hard” (or “semi-soft”) in that they are estimates based on present conditions. For the “soft” parameters, we make an educated guess. In [Table I](#), values of the hard, semi-hard, and soft parameters are tabulated.

In a manner similar to [Welander \(1982\)](#), the coefficients  $h$ ,  $h_{so}$ ,  $h_{gl}$ , and  $\epsilon_e$  for present conditions are found assuming steady state conditions for the system of [Eq. \(18\)](#). We assume that in [\(18e\)](#),  $T_g$  is in equilibrium at  $T_m$ . There are then four equations and four unknowns for the equilibrium calculation.

Our model is low dimensional and will produce relaxation oscillations. There are other such models to which we can roughly compare. [Saltzman et al. \(1981\)](#) is a two dependent variable (sine of latitude of ice mass and ocean temperature) model postulated from somewhat crude but plausible heuristic estimates of feedback terms yielding oscillations. We will see that our model can be reduced to one with similar dependent variables. The textbook of [Saltzman \(2002\)](#) has a much more developed model. This three variable (ice volume, deep ocean temperature, and carbon cycle) appears to be the best of the relaxation models. It is best in the sense that the physical basis is strongly supported, and the results are reasonable. A concise description of the model is given

TABLE I. Nominal values of hard, semi-hard and soft parameters. [The extra subscript  $i$  denotes a value based on present conditions from [Peixoto and Oort \(1992\)](#) or [Trenberth \(1992\)](#)].

Hard parameters	
$\sigma = 5.7 \times 10^{-8} \text{ W m}^{-2} \text{ K}^{-4}$	$P_p = 22 \text{ kyrs}$
	$P_o = 41 \text{ kyrs}$
$L_s = L_g = 334 \text{ J g}^{-1}$	$P_e = 100 \text{ kyrs}$
$L_{ev} = 2501 \text{ J g}^{-1}$	$S_c = 1360 \text{ W m}^{-2}$
$L_v = 2835 \text{ J g}^{-1}$	$T_f = 271 \text{ K}$
Semi-hard parameters	
$\delta_g = 2280 \text{ m}$	$V_w = 0.71 \delta_o s$
$\delta_s = 2 \text{ m}$	$T_{oqi} = 300 \text{ K}$ $B = (\dot{m}_{gi}/s)/\alpha_{oi}\alpha_{gi}F_w(T_{oi})$
	(so $T_{oi} = 292.2 \text{ K}$ )
$\delta_o = 3800 \text{ m}$	$T_{li} = 298 \text{ K}$ $\dot{m}_{gi}/s = 1.7 \times 10^{-4} \text{ g m}^{-2} \text{ s}^{-1}$
	(so $T_{li} = 290.1 \text{ K}$ )
$\alpha_{gi} = 0.03$	$A_{gi} = A_{si} = 0.9$ $b_p = 1.25\pi/180$
$\alpha_{si} = 0.048$	$A_{oi} = 0.15$ $b_o = b_p$
$\alpha_{oi} = 0.71$	$A_{li} = 0.23$ $b_e = \frac{2}{3} b_p$
Soft parameter estimates	
$\bar{\delta}_l = 100 \text{ m}$	$T_m = T_{gi} = 260 \text{ K}$ $a = 2.3$

in [Chap. 15](#) where much of the prior fourteen chapters are devoted to physically justifying the model. One similarity is that the ice mass is essentially that of the northern hemisphere.

Another model is that of [Paillard and Parrenin \(2004\)](#), which is applied to Antarctica. It also has three variables, ice mass, area of glacier, and  $\text{CO}_2$  concentration, but distinctively does not have temperature as a dependent variable. A similarity with our model is the use of the step function to represent a rapid change. However, whereas ours is a change in heat flow, theirs is a change in the carbon cycle. Finally, there is the “minimal model for ice ages” of [Crucifix \(2011\)](#) where the well known van der Pol oscillator is adapted to the ice mass oscillation data. A virtue of such a simple model is that it can easily be used to investigate various kinds of synchronization to the forcing ([de Saedeleer et al., 2013](#)) and used to investigate chaos ([Matsui and Aihara, 2014](#)). We will see that our model can be reduced to something similar and could be further analyzed in a like manner.

The bases of our model are different than the above models. In comparison to the models of [Saltzman et al. \(1981\)](#) and [Crucifix \(2011\)](#), the terms of the system of equations of our model are not basically heuristic to obtain a realistic result, but have an understandable physical basis. On the other hand, the physical basis of the system of [Saltzman \(2002\)](#) is more physically justified. We do not expect our model to challenge a more sophisticated model such as [Saltzman \(2002\)](#) in its physical conformity to nature.

#### IV. RESULTS AND DISCUSSION

For values exactly as those given in [Table I](#) except with no external orbital forcing, the equilibrium state yields values for unknown parameters:  $\epsilon_{eo} = 0.67$ ,  $h = 5.94$ ,  $h_{so} = 31.22$ , and  $h_{gl} = 13.84$ . (The temperature of the glacier,  $T_g$ , equals  $T_m$ , and remains constant in time and, hence, [Eq. \(18e\)](#) is not necessary and there is one less equation in the system.) In examining the system, we will hold fixed all the parameters so far specified and only vary the coefficients of the effective emissivity,  $\epsilon_e$ , from [\(14\)](#) and of the ocean albedo,  $A_o$  (and correspondingly that of the land,  $A_l$ ), from [\(15\)](#). If the system is weakly perturbed, by changing  $\epsilon_T$  to  $-0.01$  (with  $\epsilon_\alpha$ ,  $A_T$ ,  $A_\alpha$  remaining 0), the system remains in stable equilibrium and remains stably oscillating with a small amplitude if the external orbital forcing is applied. These results are not very interesting, though they are somewhat reassuring.

If we perturb more strongly with  $\epsilon_T = -0.1$ ,  $\epsilon_\alpha = 0.0$ ,  $A_T = 0.1$ ,  $A_\alpha = 0.1$ , and no forcing, we lose all the ice and get a less comforting warmer ocean temperature,  $T_o$ . If  $\epsilon_T$  is decreased more, the ocean eventually boils. In fact, the parameters can be manipulated to get the two extremes: boiling ocean or snowball earth.

Things get much more interesting when we let the albedo of the ocean ( $A_o$ ) decrease with an increase of the glacier area (i.e.,  $A_\alpha < 0$ ). For  $\epsilon_T = -0.0094$ ,  $\epsilon_\alpha = 0.0$ ,  $A_T = 0.0$ ,  $A_\alpha = -0.67$ , and with no external periodic forcing, we get oscillations. [Figure 2](#) shows the results for this case. We get natural oscillations as shown in [Fig. 2\(a\)](#), which



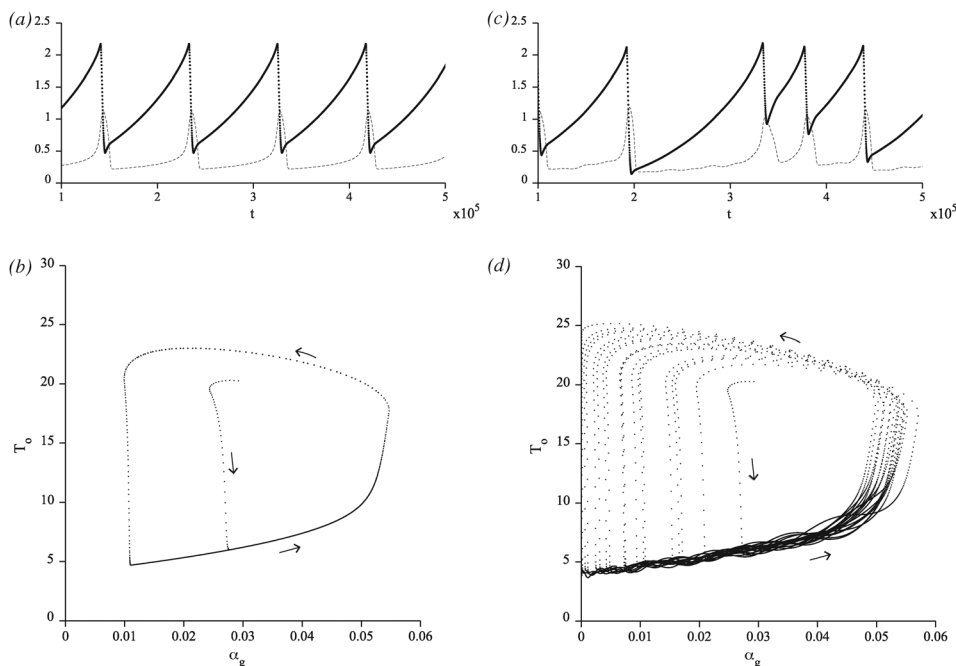


FIG. 2. Results for the model for the parameters  $\epsilon_T = -0.0094$ ,  $\epsilon_x = 0$ , and  $A_T = 0$ ,  $A_x = -0.67$ . (a) and (c) The evolution over 400kyrs of normalized glacier extent ( $\frac{\alpha_g}{\alpha_{gi}}$ ) (solid and dots) and normalized ocean temperature ( $\frac{T_o - 273}{T_{oi} - 273}$ ) (dashed) where (a) is without orbital forcing and (c) with orbital forcing. (b) and (d) Phase plot of ocean temperature ( $T_o$ ) versus glacier extent ( $\alpha_g$ ) where (b) is without orbital forcing and (d) is with orbital forcing. The trajectories are counterclockwise (as shown by the arrows) and the dots on the trajectory are 100 years apart, so that the “fast” dotted portion of the cycle can be distinguished from the “slow” solid portion.

shows the evolution of normalized values of the glacier extent ( $\frac{\alpha_g}{\alpha_{gi}}$ ) (solid and dots) and the ocean temperature ( $\frac{T_o - 273}{T_{oi} - 273}$ ) (dashed). It shows the saw toothed oscillations, which are characteristic of the data with a slow buildup of ice followed by swift melting. However, the data show the temperature slowly decreasing and then swiftly increasing, and here the model does the opposite. The oscillations can be tuned by varying the parameters but not changed much if oscillations are to result. For example, we get oscillations only for  $\epsilon_T = -0.0094 \pm 0.004$  with the period varying from about 30 to 130kyrs as  $\epsilon_T$  increases. The value 0.0094 was chosen to give an approximately 100kyr period as shown in the actual data. But it was found that, if any oscillations result, they will have a period of order 100kyrs. With all the other parameters fixed, an increase in the magnitude of  $A_x$  decreases the period.

For the same parameters, Fig. 2(b) shows a limit cycle on a phase diagram of  $T_o$  vs.  $\alpha_g$ . The trajectory on the limit cycle is counterclockwise as shown by the arrows. Each dot on the trajectory represents 100 years in elapsed time. So the “fast” part is where the dots are spread out and the “slow” the solid line. The trajectory from the point of minimum ice mass ( $\alpha_g \simeq 0.01$ ,  $T_o \simeq 21^\circ\text{C}$ ) counterclockwise to the point of maximum ice mass ( $\alpha_g \simeq 0.055$ ,  $T_o \simeq 17.8^\circ\text{C}$ ) is characterized by heat transferred to the ice [ $H_g$  from (18a)] being negative, while on the remainder of the trajectory back to the minimum ice mass point, it is positive. Where  $H_g < 0$ , there is ice growth due to precipitation, which is a relatively slow process. The saw tooth pattern is formed by the “slow” growth followed by the “fast” melt, sharply produced by a change in the sign of the argument of the step function,  $U(H_g)$ , in (18a). The maximum ice mass is reached before the maximum temperature, but the maximum ice mass is reached at a relatively high temperature. This result appears not to conform to reality. The spectrum (not shown) is like a

typical nonlinear oscillator with the period of the fundamental spike being about 88kyrs and the other spikes of diminishing amplitude being integer multiples of the fundamental frequency. Plots (not shown) of  $T_o$  vs.  $T_L$  and  $T_o$  vs.  $\alpha_s$  show that both  $T_L$  and  $\alpha_s$  can be approximated as functions of  $T_o$ . This demonstrates why we can state that the system can be approximated with just the two dependent variables,  $\alpha_g$  and  $T_o$  similar to one of the Saltzman models (Saltzman *et al.*, 1981).

It should be emphasized that we do not get oscillations unless the effective emissivity ( $\epsilon_e$ ) decreases with increasing temperature ( $T_o$ ) (i.e.,  $\epsilon_T < 0$ ) and the effective ocean albedo ( $A_o$ ) decreases with increasing glacier extent ( $\alpha_g$ ) (i.e.,  $A_x < 0$ ). Since the amount of water vapor in the air increases with temperature, it makes sense that  $\epsilon_e$  would decrease with increased temperature. However, why there might be an effect of  $\alpha_g$  on  $A_o$  is not obvious. Would more ice have the effect of decreasing water vapor, thus clouds, over the ocean? And does decreasing clouds decrease the effective albedo? For this model to produce oscillations, the answers would seem to have to be yes.

Now let us include the Milankovitch forcing for the conditions of Fig. 2. As shown in Fig. 2(c), the glacier and temperature evolutions appear to be randomly periodic. The phase diagram, Fig. 2(d), shows that the system is now mildly chaotic and the spectrum (not shown) also shows chaos. This is not unexpected. An autonomous two dependent variable nonlinear system would not be chaotic. But the addition of forced oscillations would introduce the possibility.

The chaotic behavior can be increased by changing the parameters. For  $\epsilon_T = -0.008$ ,  $\epsilon_x = 0.0$ ,  $A_T = 0.0$ , and  $A_x = -0.33$ , we see that glacier and temperature evolutions, Fig. 3(a), look more chaotic and the phase diagram, Fig. 3(b), really looks chaotic (the “moth” effect). The spectrum (not shown) appears chaotic, but all the forcing frequencies stand out, as compared to the spectra for the previous conditions. Interestingly, if the external forcing is removed, the

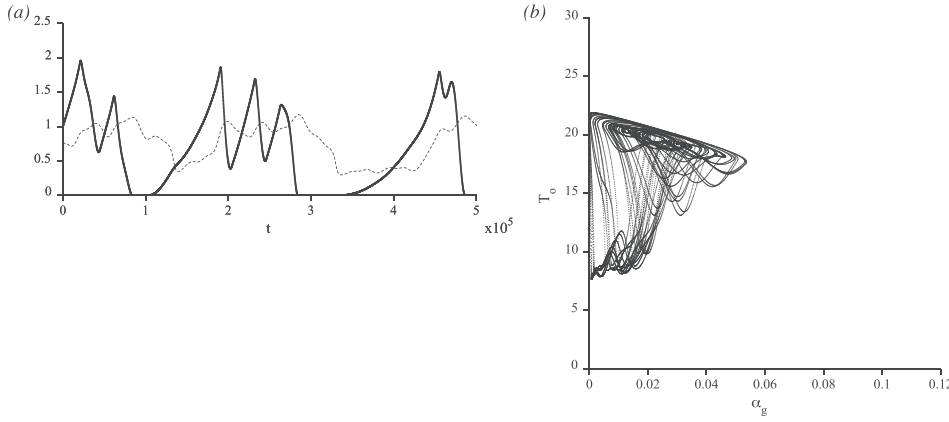


FIG. 3. Results for the model for the parameters  $\epsilon_T = -0.008$ ,  $\epsilon_x = 0$ ,  $A_T = 0$ , and  $A_x = -0.33$  with orbital forcing. (a) Evolution over 500kyrs of normalized glacier extent ( $\frac{x_g}{x_{gi}}$ ) (solid and dots) and normalized ocean temperature ( $\frac{T_o - 273}{T_o - 273}$ ) (dashed). (b) Phase plot of the ocean temperature ( $T_o$ ) versus glacier extent ( $\alpha_g$ ). External forcing kicks a stable solution into a chaotic unstable flow.

system is stable, non-oscillating. However, it is barely stable, and the forcing knocks it out of this stability, an excitable system as described by Crucifix (2012).

What we have done thus far is an analysis of what can be called the original full model. We have alluded to the fact that the temperature evolution does not seem to be realistic. In the following section we will address this situation and present a modification to rectify it.

## V. A TRUNCATED MODEL AND DISCUSSION

As mentioned in previous section,  $T_o$  and  $T_l$  approximately correlate and the same goes for  $T_o$  and  $\alpha_s$ . Also  $T_g$  is constant and equal to  $T_m$ . Thus in a neighborhood of parameter space, we can eliminate  $T_g$ ,  $T_l$ , and  $\alpha_s$ , leaving only  $T_o$  and  $\alpha_g$  as dependent variables. We assume an approximate linear fit with a positive slope for  $T_l$  vs.  $T_o$  and a linear fit with a negative slope for  $\alpha_s$  vs.  $T_o$ . The simpler system then consists of essentially Eqs. 18(a) and 18(c).

The equation for the rate of change of the glacier (18a) is especially revealing. If we rewrite (18a) in terms of the time scale of glacier growth,  $\tau_g = \alpha_{gp} \delta_g / \left( \frac{\dot{m}_{gp}}{s} C_1 \right)$ , in the first term, and the time scale of glacier melt,  $\tau_m = \delta_g L_g \alpha_{gp} / H_{gp} C_1$ , in the second term, we obtain

$$\frac{d\alpha_g}{dt} = \left[ \frac{1}{\tau_g} \frac{F_w \alpha_o}{F_{wp} \alpha_{op}} - \frac{1}{\tau_m} \frac{H_g \alpha_{gp}}{H_{gp} \alpha_g} U(H_g) \right] \alpha_g, \quad (20)$$

where  $\alpha_{gp}$ ,  $\alpha_{op}$ ,  $F_{wp}$ , and  $H_{gp}$  are these quantities at nominal conditions. For nominal values,  $\tau_g$  is of order of 10kyrs and  $\tau_m$  is of order of 1kyrs. Thus, the growth of the glacier is much less in magnitude than the melting of the glacier. However, the melting term is zero when the net heat transfer to the glacier,  $H_g$ , is negative. The ratio of  $\tau_g$  to  $\tau_m$  is large and we will see that this is the large parameter for a relaxation oscillation.

More specifically, let us consider the following ‘‘boiled down,’’ two-dependent variable model

$$\frac{d\alpha_g}{dt} = \frac{C_1}{\delta_g} \left[ BF_w \alpha_g - \frac{\overline{H}_g}{L_g} \alpha_g U(\overline{H}_g) \right], \quad (21a)$$

$$\frac{dT_o}{dt} = \frac{C_2}{\delta_o} \overline{H}_o, \quad (21b)$$

where

$$\overline{H}_g = \frac{S_c}{4} (1 - A_g) \left( 0.74 \alpha_g \frac{\beta_a}{\beta_{ao}} \right) - \epsilon_e \sigma T_m^4 + h(T_o - T_m)$$

and

$$\overline{H}_o = \frac{S_c}{4} (1 - A_o) \left( 1 - 0.74 \alpha_g \frac{\beta_a}{\beta_{ao}} \right) - \epsilon_e \sigma T_o^4 - h \alpha_g (T_o - T_m).$$

Here we have neglected the equations for  $\alpha_s$ ,  $T_l$ ,  $T_g$ , and assumed that  $\alpha_o = 1$ , only one heat transfer coefficient,  $h$ , and neglected the latent heat terms. We can show that the projection area,  $A_c$ , from (11) can be approximated as  $0.74 \alpha_g$  for  $\alpha_g \lesssim 0.1$ . As before, the variables  $\epsilon_e$  and  $A_o$  are given by (14) and (15) and  $\epsilon_{ei}$  and  $h$  are found from (21) at equilibrium.

The limit cycle for the typical solution for (21) is very much like that of the original system. Figure 4 shows a typical limit cycle solution for (21) along with the nullclines for conditions such that the natural period is about 70kyrs. The

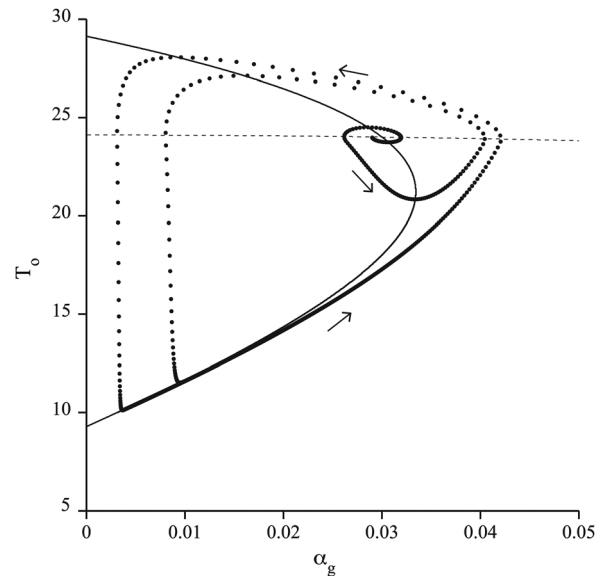


FIG. 4. Typical limit cycle for ocean temperature ( $T_o$ ) versus glacier extent ( $\alpha_g$ ) for the truncated system [Eq. (21)] with no orbital forcing. The thick solid line and big dots are the trajectory of the solution. The thin solid line is the  $T$ -nullcline and the dashed line the  $\alpha$ -nullcline. The trajectory spirals counterclockwise out from the equilibrium to the limit cycle (as shown by the arrows). The elapsed time between big dots is 100 years, so slower and faster parts of the trajectory are distinct.

solution trajectory, represented by the thicker solid line and dots, spirals counterclockwise (as shown by the arrows) out from the unstable focus to the limit cycle. The gap between these dots represents 100 years. The  $\alpha$ -nullcline ( $\frac{d\alpha_g}{dt} = 0$ ) is represented by the dashes and the T-nullcline ( $\frac{dT_o}{dt} = 0$ ) by the thinner solid line. The intersection of these nullclines is of course the equilibrium point. We see that  $\frac{d\alpha_g}{dt}$  changes sign every time the trajectory crosses the  $\alpha$ -nullcline and similarly that  $\frac{dT_o}{dt}$  changes sign when crossing the T-nullcline. If you begin on the most rightward point on the trajectory on the limit cycle, you are on the  $\alpha$ -nullcline. Since on the right side of Eq. (21), the right term (melting) is so much greater than the left (growth), the  $\alpha$ -nullcline is essentially where  $\bar{H}_g$  changes sign and is only weakly dependent on  $\alpha_g$ , approximated by the line  $T_o = 24^\circ\text{C}$ . Since this most rightward point is to the right of the T-nullcline where  $T_o$  must increase, the trajectory moves into the region above the  $\alpha$ -nullcline where  $H_g > 0$  and  $\frac{d\alpha_g}{dt}$  is strongly negative. The glacier melts quickly ( $\alpha_g$  decreasing) with  $T_o$  continuing to increase until the trajectory crosses the T-nullcline where  $\frac{dT_o}{dt}$  becomes negative.  $T_o$  then decreases and crosses the  $\alpha$ -nullcline where  $H_g$  becomes negative and the melting term is turned off. Thus,  $\frac{d\alpha_g}{dt}$  is then very small and positive for all points below the  $\alpha$ -nullcline (the slow glacier growth due to precipitation). The temperature continues to quickly decrease with a little change in  $\alpha_g$  until the T-nullcline is encountered. The trajectory is then constrained to follow closely just below and to the right of the T-nullcline until it gets close to the vertex of the T-nullcline where it must continue to bear to the right because  $\frac{d\alpha_g}{dt}$  is still positive. We then return to the  $\alpha$ -nullcline completing one cycle. Thus, the trajectory shows the characteristics of a relaxation oscillation with the ratio of the growth times,  $\frac{\tau_g}{\tau_m}$ , being the large parameter.

As with the original model, the evolutions of the temperature and glacier extent increase and decrease together. This does not seem to correspond to the proxy data. We can more easily investigate this problem with this simpler model, especially if we simplify it even more, by linearizing all the non-linear coefficients such as  $T_o^4$  and  $F_w$  about the equilibrium point. Thus, we obtain the form:

$$\frac{dx}{dt} = q_1 [(a + by)x/\tau_g - \bar{H}_g U(\bar{H}_g)/\tau_m], \quad (22a)$$

$$\frac{dy}{dt} = q_2 [Ax^2 + Bxy + Cy^2 + Dx + Ey + F], \quad (22b)$$

where  $x = \alpha_g/\alpha_{gi}$  and  $y = (T_o - 273)/(T_{oi} - 273)$ , and  $\bar{H}_g = cx^2 + dy + e$ . The parameters a, b, c, d, e, A, B, C, D, E, F,  $q_1$ , and  $q_2$  are functions of the original parameters. The local stability at the equilibrium point can straightforwardly be investigated showing bifurcations from saddle points and stable and unstable spirals, but we will leave this to future investigation. We are most interested in the global properties of the limit cycle.

Equation (22b) shows that the T-nullcline is a conic section which we see from Fig. 4 is the left branch of a hyperbola with the axis essentially parallel to the  $\alpha_g$ -axis. The slope of the lower branch of this hyperbola is positive and, as long as this is so,  $T_o$  and  $\alpha_g$  will increase together which we think is not realistic. So let us make this slope negative by manipulating the constants A, B, C, D, and E in the T-nullcline equation to rotate and translate the hyperbola to make this slope negative. This rotation is shown on the phase plot in Fig. 5(a). Figure 5(b) for the evolution of the temperature (dashed line) shows the kind of behavior we think is realistic. However, this result is a mathematical artifact (a nonphysically justified twist). This is somewhat like the model of Crucifix (2011) where a simple van der Pol oscillator is contorted to behave like the climate. The question is can the original parameters of our model be chosen in a realistic way to give this result? The answer seems to be no.

So what is to be done? Let us reconsider our model of the atmosphere, which in our case is the effective emissivity ( $\epsilon_e(\alpha_g, T_o)$ ) and effective ocean albedo [ $A_o(\alpha_g, T_o)$ ], which come into the model through Eqs. (14) and (15). These equations are essentially the linear approximations about the equilibrium of these unknown functions representing the black box of the atmosphere. So let us go to a higher approximation, the Taylor series to the second order about the equilibrium point.

$$\begin{aligned} \epsilon_e(\alpha_g, T_o) = & \epsilon_{ee} + \epsilon_T(T_o - T_{oi}) + \epsilon_\alpha(\alpha_g - \alpha_{gi}) \\ & + \frac{1}{2!} \{ \epsilon_{TT}(T_o - T_{oi})^2 + 2\epsilon_{\alpha T}(T_o - T_{oi}) \\ & \times (\alpha_g - \alpha_{gi}) + \epsilon_{\alpha\alpha}(\alpha_g - \alpha_{gi})^2 \}, \end{aligned} \quad (23)$$

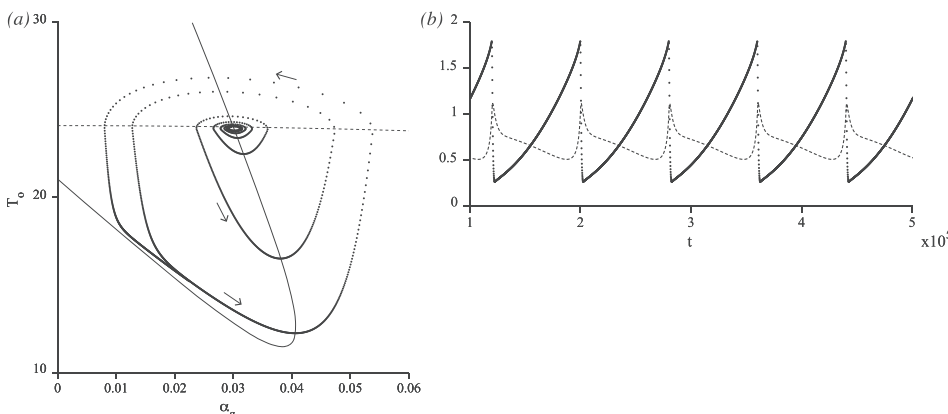


FIG. 5. Truncated model with a non-physical rotation of T-nullcline. (a) Typical phase plot of the ocean temperature ( $T_o$ ) versus glacier extent ( $\alpha_g$ ) of the system of Eq. (22). The solution trajectory is the big dots. The T-nullcline is the thin line and the  $\alpha$ -nullcline is the dashed. (b) Evolution over 400kyrs of normalized glacier extent ( $\frac{\alpha_g}{\alpha_{gi}}$ ) (solid and dots) and normalized ocean temperature ( $\frac{T_o - 273}{T_{oi} - 273}$ ) (dashed), corresponding to (a), showing a more realistic behavior for the temperature.

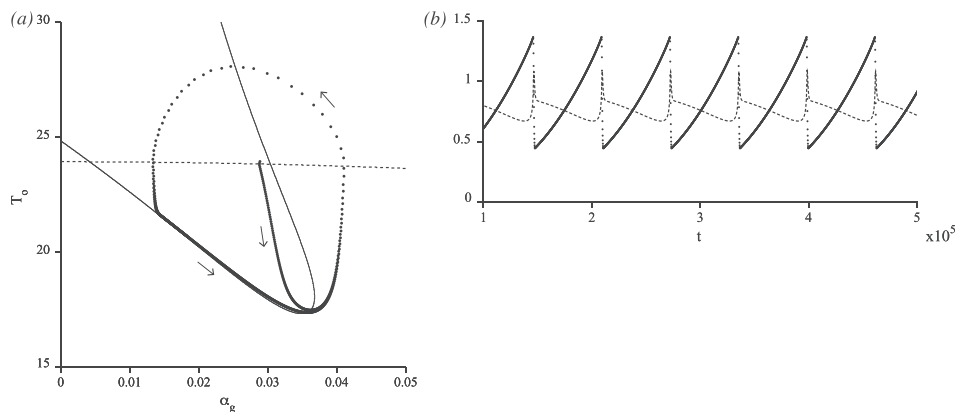


FIG. 6. Truncated model of the system of Eq. (21) with a rotation of the T-nullcline that is physically justified, using Eqs. (23) and (24). The parameters are  $\epsilon_T = -0.01$ ,  $A_x = -2.1$ ,  $\epsilon_{xT} = -0.16$ ,  $A_{xx} = -66.0$  and the rest of the partials zero. (a) The phase plot of the ocean temperature ( $T_o$ ) versus glacier extent ( $\alpha_g$ ) showing the counterclockwise trajectory (solid line and big dots in the direction of the arrows). The T-nullcline is the thin line and the  $\alpha$ -nullcline is the dashed. (b) Evolution over 500kyrs of normalized glacier extent ( $\frac{\alpha_g}{\alpha_{gi}}$ ) (solid and dots) and normalized ocean temperature ( $\frac{T_o - 273}{T_o - 273}$ ) (dashed), corresponding to (a), showing the behavior of the temperature which we want to see legitimately from the model.

$$\begin{aligned}
 A_o(\alpha_g, T_o) = & A_{oi} + A_T(T_o - T_{oi}) + A_x(\alpha_g - \alpha_{gi}) \\
 & + \frac{1}{2!} \left\{ A_{TT}(T_o - T_{oi})^2 + 2A_{xT}(T_o - T_{oi}) \right. \\
 & \left. \times (\alpha_g - \alpha_{gi}) + A_{xx}(\alpha_g - \alpha_{gi})^2 \right\}, \quad (24)
 \end{aligned}$$

where now the partial derivatives evaluated at the equilibrium,  $\epsilon_T$ ,  $\epsilon_x$ ,  $\epsilon_{TT}$ ,  $\epsilon_{xT}$ ,  $\epsilon_{xx}$ ,  $A_T$ ,  $A_x$ ,  $A_{TT}$ ,  $A_{xT}$ ,  $A_{xx}$  are free parameters. Thus, though we do not explicitly have an atmosphere in the model, we can shape the functions  $\epsilon_e(\alpha_g, T_o)$  and  $A_o(\alpha_g, T_o)$  which indirectly represent the atmosphere. This does work. Figures 6(a) and 6(b) show the results using (23) and (24) in the boiled down system (21) with  $\epsilon_T = -0.01$ ,  $A_x = -2.1$ ,  $\epsilon_{xT} = -0.16$ ,  $A_{xx} = -66.0$ , and the rest of the partials zero. Figure 6(a) shows the rotated T-nullcline that is desired and Fig. 6(b) shows that temperature now behaves in the desired fashion. As we might expect, the cross derivative  $\epsilon_{xT}$  makes the difference. Thus, we have shown that the atmosphere, as represented by the functions (23) and (24), behaves nonlinearly as might be expected.

Now let us go back to the original full model [Eqs. (18) and (19)] using Eqs. (23) and (24) instead of (14) and (15) and including external forcing. Figures 7(a) and 7(b) show that the original model with external forcing is also made more realistic where in this case  $\epsilon_T = -0.01$ ,  $A_x$

$= -2.1$ ,  $\epsilon_{xT} = -0.16$ ,  $A_{xx} = -56.0$ ,  $A_{xT} = -0.07$  with the rest of the partials zero. This is the most realistic result of this model to date. Interestingly, one of the critiques of Saltzman’s three variable model (Crucifix, 2012) is that the interesting dynamics are in the equation for the carbon cycle which is not well known. The carbon cycle equation represents the atmosphere in Saltzman’s model. Analogous to this for our model is the dependence of the dynamics on the black box atmosphere represented by the equations for  $\epsilon_e$  and  $A_o$  [Eqs. (23) and (24)]. In essence, we are building initially unknown nonlinear functions that represent the atmosphere in our model. It is not surprising that initially using linear functions would not be good enough.

### VI. SUMMARY AND CONCLUSIONS

Though motivated as a modeling exercise, this rather crude, lumped parameter system gives interesting results. For values of the parameters near nominal, the unforced system is very sensitive, yielding equilibrium, a big freeze, a big melt, and steady oscillations with small changes in the parameters. The data of the past million years are dominated by oscillations so we are most interested in oscillating results. Around a particular point in parameter space, the system can be truncated down to just two dependent variables

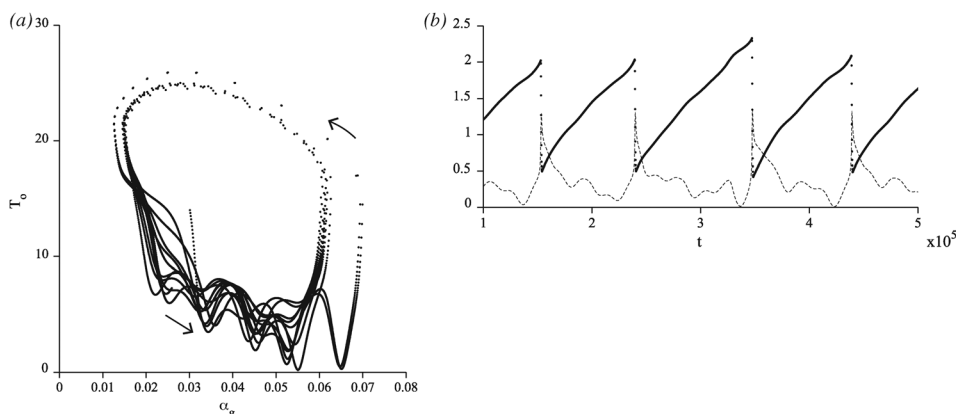


FIG. 7. The original full model with orbital forcing, where the parameters from Eqs. (23) and (24) are  $\epsilon_T = -0.01$ ,  $A_x = -2.1$ ,  $\epsilon_{xT} = -0.16$ ,  $A_{xx} = -56.0$ ,  $A_{xT} = -0.07$ , and the rest of the partials zero. (a) Typical phase plot of the ocean temperature ( $T_o$ ) versus glacier extent ( $\alpha_g$ ) where the trajectory is counterclockwise (in the direction of arrows). (b) Evolution over 400kyrs of normalized glacier extent ( $\frac{\alpha_g}{\alpha_{gi}}$ ) (solid and dots) and normalized ocean temperature ( $\frac{T_o - 273}{T_o - 273}$ ) (dashed), corresponding to (a). This is probably the most realistic behavior of the model.

and still yields its basic response—a relaxation oscillation. The key to getting oscillations is having the effective emissivity decreasing with temperature and, at the same time, the effective ocean albedo decreases with increasing glacier extent. We get natural oscillations of periods of order of 100kyrs unrelated to the Milankovitch forcing. When the forcing is applied, the system becomes chaotic.

The original model results are realistic for the ice mass variation, but not for the temperature. However, we found that by using a nonlinear modification of the functions ( $\epsilon_e$  and  $A_o$ ) representing the effect of the atmosphere, we can obtain results that are more consistent with reality. That this effect has to be nonlinear is not surprising. A salient result is that the model supports the plausibility that the 100kyr dominant period is basically a natural period of the system. This result supports the opinion of Saltzman (1990) that the dominant 100kyr period is a result of nonlinear dynamics. Since the system is chaotic, we might expect time spans when a 100kyr period is apparent and spans when it is not.

Much more can be done in investigating the relaxation oscillation dynamics of the model. The uniqueness of this model is its relative simplicity while yielding good results. As such, the parameters are physically transparent. This should make the model conducive to a marriage with a biological model investigating the effect of biota on albedo and subsequently on the dynamics. This brings us back to the spirit of “Daisyworld.”

Bathiany, S., Dijkstra, H., Crucifix, M., Dakos, V., Brovkin, V., Williamson, M. S., Lenten, T. M., and Scheffer, M., “Beyond bifurcation: Using complex models to understand and predict abrupt climate change,” *Dyn. Stat. Clim. Syst.* **1–31**, dzw004 (2016).

Berger, A. and Loutre, M. F., “Insolation values for the climate of the last 10 million years,” *Quaternary Science Reviews* **10**(4), 297–317 (1991).

Broecker, W. S., *The Glacial World According to Wally* (Eldigio Press, Palisades New York, 1993).

Crucifix, M., “How can a glacial inception be predicted?,” *Holocene* **21**, 831–842 (2011).

Crucifix, M., “Oscillators and relaxation phenomena in Pleistocene climate theory,” *Philos. Trans. R. Soc. A* **370**, 1140–1165 (2012).

Crucifix, M. and Rougier, J., “On the use of simple dynamical systems for climate predictions: A Bayesian prediction of the next glacial inception,” *Eur. Phys. J. Spec. Top.* **174**, 11–31 (2009).

de Saedeleer, B., Crucifix, M., and Wiczorek, S., “Is the astronomical forcing a reliable and unique pacemaker for climate? A conceptual model study,” *Clim. Dyn.* **40**, 273–294 (2013).

Hansen, J. and Sato, M., *Earth’s Climate History: Implications for Tomorrow* (NASA Science Briefs, 2011).

Hays, J. D., Imbrie, J., and Shackleton, N. J., “Variation in Earth’s orbit: Pacemaker of the ice ages,” *Science* **194**, 1121–1132 (1976).

Matsui, T. and Aihara, K., “Dynamics between order and chaos in conceptual models of glacial cycles,” *Clim. Dyn.* **42**, 3087–3099 (2014).

Paillard, D. and Parrenin, F., “The Antarctic ice sheet and the triggering of deglaciations,” *Earth Planet. Sci. Lett.* **227**, 263–271 (2004).

Peixoto, J. P. and Oort, A. H., *Physics of Climate* (American Institute of Physics, New York, 1992).

Posmentier, E. S., “Periodic, quasiperiodic and chaotic behavior in a nonlinear toy climate model,” *Ann. Geophys.* **8**, 781–790 (1990).

Saltzman, B., “Three basic problems of paleoclimatic modeling: A personal perspective and review,” *Clim. Dyn.* **5**, 67–78 (1990).

Saltzman, B., *Dynamical Paleoclimatology: Generalized Theory of Global Climate Change* (Academic Press, New York, 2002).

Saltzman, B., Hansen, A. R., and Maasch, K. A., “The late quaternary glaciations as the response of a three-component feedback system to Earth-orbital forcing,” *J. Atmos. Sci.* **41**, 3380–3389 (1984).

Saltzman, B., Sutera, A., and Evenson, A., “Structural stochastic stability of a simple auto-oscillatory climatic feedback system,” *J. Atmos. Sci.* **38**, 494–503 (1981).

Saunders, P. T., “Evolution without natural selection: Further implications of the Daisyworld parable,” *J. Theor. Biol.* **166**, 365–373 (1994).

Toner, M. and Kirwan, Jr., A. D., “Periodic and homoclinic orbits in a toy climate model,” *Nonlinear Processes Geophys.* **1**, 31–40 (1994).

Trenberth, K. E., *Climate System Modeling* (Cambridge University Press, New York, 1992).

Tziperman, B., Raymo, M. E., Huybers, P., and Wunch, C., *Paleoceanography* **21**, PA4206, doi:10.1029/2005PA001241 (2006).

Watson, A. J. and Lovelock, J. E., “Biological homostasis of the global environment: The parable of Daisyworld,” *Tellus* **35B**, 284–289 (1983).

Welander, P., “A simple heat-salt oscillator,” *Dyn. Atmos. Oceans* **6**, 233–242 (1982).

Wood, A. J., Ackland, G. J., Dyke, J. G., Williams, H. T. P., and Lenton, T. M., “Daisyworld: A review,” *Rev. Geophys.* **46**, RG1001, doi:10.1029/2006RG000217 (2008).